

ORIGINAL RESEARCH PAPER

Machine learning-driven approach to quantify the beach susceptibility to storm-induced erosion

Salika Thilakarathne, Takayuki Suzuki and Martin Mäll

Department of Civil Engineering, Yokohama National University, Yokohama, Japan

ARTICLE HISTORY

Compiled November 24, 2023

ABSTRACT

Evaluating beach vulnerability requires assessing both susceptibility and recovery potential. This study focuses on quantifying the susceptibility of sandy beaches to storm-induced erosion by analyzing 14 key morphometric indicators. The data set used spans 24 years and includes morphological and metocean data, enabling the identification of 347 storms and their corresponding beach responses. The analysis of pre-storm beach profiles revealed four distinct patterns: unbarred, inner sandbar, outer sandbar, and double sandbar profiles. XGBoost models were trained for each profile pattern, utilizing the 14 morphometric indicators as input and shoreline change as output. SHAP feature importance analysis was employed to determine the most influential morphometrics. The results revealed that the morphometrics contributing to beach susceptibility vary depending on the beach profile type. Notably, the initial shoreline position plays a significant role in unbarred and double sandbar profiles. Storm cases were divided into three groups based on storm power to validate the beach erosion susceptibility number (BESN). Evaluation of BESN for each profile pattern and storm group showed that unbarred profiles under average storm conditions exhibited the highest correlation, with a Pearson correlation coefficient (r) of 0.75. There was at least a 0.40 correlation coefficient between observed beach erosion and BESN in eight of the 12 scenarios studied. These findings highlight the effectiveness of BESN in quantifying the susceptibility of different beach profile patterns to erosion. BESN provides valuable insights regarding the vulnerability of sandy beaches by considering key morphometric indicators and assisting in coastal management and decision-making processes.

KEYWORDS

Beach erosion; beach vulnerability; coastal storms; sandy beaches; SHAP explanation method; XGBoost

1. Introduction

A natural beach zone is considered a valuable asset that provides economic and environmental benefits to the local community. The beach and its natural beauty must be protected from destructive human activities, climate change-related hazards, and extreme weather conditions. Frequent natural hazards to beach zones often cause instabilities to their long-term profile migrations both landward and seaward (Turner et al. 2016). The seasonal response of a beach involves many complex coastal processes, and holistic approaches are commonly used to understand the vulnerability of coastal regions, especially focusing on climate change-driven factors (Kantamaneni et al. 2017,

2018). Although discussions on coastal vulnerability have been ongoing since 1991, only a few coastal vulnerability studies have focused on risk-related concepts specific to the beach zone.

Alexandrakis and Poulos (2014) first tried to quantify the beach vulnerability using key morphological and metocean data elements. They focused on sediment transport mechanisms, effect of sea level rise, and land-form characteristics to numerically approximate the beach vulnerability. Several studies investigated the characteristics of coastal processes to assess beach zone vulnerability to hazards such as erosion, sea level rise, and flooding (de Andrade, Sousa, and Siegle 2019; Kim, Lim, and Lee 2021; Thilakarathne et al. 2022; Thilakarathne, Suzuki, and Mll 2023). Kim, Lim, and Lee (2021) proposed the beach recovery factor and beach response factors, which emphasize beach resilience and susceptibility to storm-induced beach erosion, respectively. However, studies addressing both susceptibility and resilience, two key aspects of vulnerability, are limited (Thilakarathne, Suzuki, and Mll 2023). Although significant research in coastal engineering has examined the influence of hydrodynamic and wave climate on beach erosion (Dean and Jr 1976; Hallermeier 1980; Dolan and Davis 1994; Callaghan et al. 2008; Pender and Karunarathna 2013; Dissanayake, Brown, and Karunarathna 2014; Eichentopf et al. 2020; Mendoza et al. 2022), there is a dearth of information regarding the morphometric characteristics of beach profiles. The discussions on specific relationships between coastal morphometrics such as sandbar formation and beach erosion exist (Ruessink and Kuriyama 2008; Pape, Kuriyama, and Ruessink 2010; Banno et al. 2020; Januait et al. 2021) and however, the risk-related vulnerability aspects are limited (Thilakarathne, Suzuki, and Mll 2023).

Many coastal vulnerability studies predominantly address the implications of sea-level rise, which is considered one of the most significant climate-related hazards under discussion today. However, the damaging impact of coastal storms on sandy beaches worldwide cannot be overlooked. These storms induced short-term fluctuations within long-term shoreline trends, spanning from seasonal to decadal or even century-scale changes (Ciavola and Coco 2017). Coastal storms, which are characterized by strong winds, high waves, and heavy rainfall, can cause significant damage to coastal landscapes (Harley 2017). During storms, waves can reach large heights, resulting in considerable beach erosion (Gallagher, Elgar, and Guza 1998; Hoefel and Elgar 2003; Ciavola and Coco 2017). Depending on the power of the storm, meters of beach width can be lost in just a few hours or days (Zhang, Douglas, and Leatherman 2002). Severe erosion occurs in particularly vulnerable areas characterized by factors such as high tides, steep gradients, and weak soils. Additionally, coastal storms contribute to the loss of sediment and vegetation, which profoundly impacts local ecosystems. Furthermore, the combination of storms and the rising sea levels due to global warming significantly amplifies the damages(Zhang, Douglas, and Leatherman 2004). To mitigate the erosion caused by coastal storms, coastal managers often employ measures such as beach nourishment, dune restoration, and the construction of seawalls and other protective structures (Dean 1991).

Beach morphometrics encompasses the physical characteristics of the coastal environment, including the shoreline position, beach width and slope, sediment properties, and profile shape (Hillyer 1996). These morphometric indicators play a pivotal role in comprehending coastal processes and the behavior of coastal systems. Coastal engineers rely on morphometric data to develop models and simulations that can predict the response of coastal environments to various stimuli like waves, tides, and storms (Hieu et al. 2020). Moreover, morphometric data inform decisions about coastal management and engineering projects, such as beach nourishment, dune restoration,

and the construction of seawalls and groins. The availability of accurate and up-to-date morphometric data is crucial for the success of coastal engineering endeavors, enabling engineers to design structures that suit the specific characteristics of the local coastal environment.

Numerous studies have addressed coastal vulnerability, exploring the vulnerability of coastlines to various hazards (Gornitz, White, and Cushman 1991; Gornitz et al. 1994; Perch-Nielsen 2010; SeongYoon and Yamaji 2015; Koroglu et al. 2019). It is common to consider vulnerability as a component of risk, alongside hazard and exposure. According to the Intergovernmental Panel on Climate Change (IPCC) (Field et al. 2011), vulnerability is defined as the degree of fragility of a system, including its capacity to cope (response capacity) under hazardous conditions. Therefore, when discussing beach vulnerability, both susceptibility and recovery potential are critical aspects. The focus of the present study is to quantify the susceptibility component of beach vulnerability.

This study has two primary objectives. The first objective is to investigate the relationship between beach morphometrics and beach erosion using machine learning algorithms, specifically XGBoost and SHAP. The second objective is to address the research gap related to beach susceptibility by proposing a susceptibility metric using the identified key morphometric indicators from the first objective. We introduce the beach erosion susceptibility number (BESN) as a robust metric for quantifying beach susceptibility to achieve these objectives. The effectiveness of BESN is evaluated during storm events along the Hasaki coast in Japan. The article is structured as follows: Section 2 provides a description of the data, Section 3 presents a comprehensive overview of the employed methods, and Section 4 presents and discusses the results of the morphometric analysis for indicator selection, which relates to the first objective. Section 5 presents and discusses the results of BESN development and its implications, addressing the second objective. Finally, Section 6 concludes by discussing the utility of BESN and highlighting the limitations for future work.

2. Data description

2.1. Study location

A 24-year data set on the morphology and metocean conditions at the Hasaki Oceanographic Research Station (HORS) in Japan is utilized for this study. HORS is located in Kamisu city of Ibaraki prefecture and is positioned at the center of a 16 km stretch of straight beach, extending from Choshi port in the south to Kashima port in the north, facing the Pacific Ocean (Fig. 1). This micro-tidal beach experiences a tidal range of 1.45 m and is oriented at a 59 counterclockwise angle from the north. Notably, HORS features a 392.0 m long pier that has been constructed perpendicular to the Hasaki coastline, enabling chronological data measurements since 1987 (Kato 1997). The Port and Airport Research Institute (PARI) manages the survey and research facilities at HORS.

2.2. Data measurements

Beach erosion was quantified using daily measurements of a 500 m cross-section obtained at 5 m intervals along the HORS pier (Suzuki and Kuriyama 2012). The positive distances represents the seaward distance perpendicular to the shore from the HORS

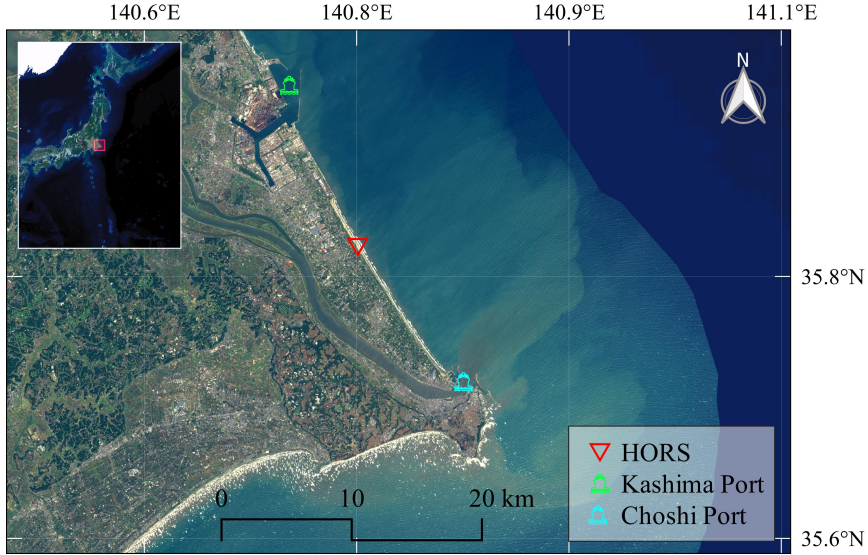


Figure 1. Location of Hasaki Oceanographic Research Station (HORS). Morphological and metocean data are collected at the 500 m long pier located at the HORS (Base map source: Geographical Survey Institute, Japan).

coordinate system origin $x=-115$. Hourly measurements of significant wave heights were recorded at 380.0 m along the HORS pier, with an average water depth of 6 m. Fig. 2 shows the variation of significant wave height over the study period. At Hasaki, the water levels relative to the datum level (Tokyo Peil +0.687 m) were as follows: the high water level was 1.25 m, the mean water level was 0.65 m, and the low water level was -0.20 m. The median sediment diameter (d_{50}) is 0.18 mm, however, intense wave conditions often result in higher d_{50} values. (Katoh 1995; Karunaratne et al. 2016; Gunaratna, Suzuki, and Yanagishima 2019). Notably, significant beach erosion is observed during the typhoon season, which spans from late August to October. In contrast, natural nourishment occurs throughout the rest of the year (Banno et al. 2020).

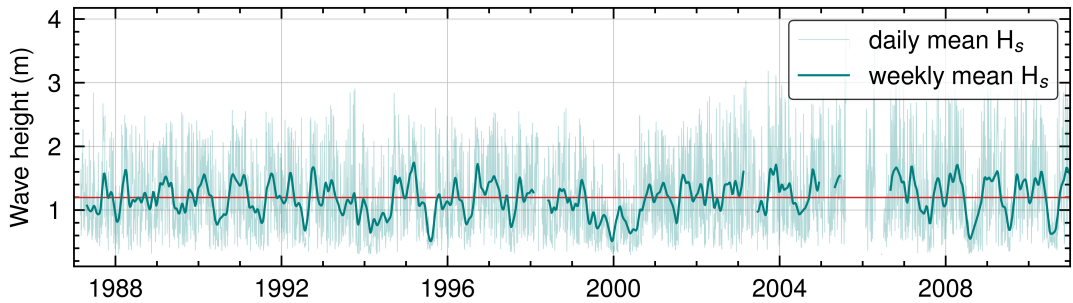


Figure 2. Daily mean and weekly mean significant wave height (H_s) at Hasaki. Thick line shows the chronological variation of weekly mean of H_s . Red horizontal line denotes the long-term mean significant wave height (1.20 m).

2.3. Storm event identification

A predefined two-threshold approach based on the Hasaki wave climate was employed to identify storms based on significant wave height (H_s) (Nagai and Ogawa 2004). A minimum storm duration (D_{min}) of 6 hours was applied to ensure the inclusion of only significant storm events (Basco and Mahmoudpour 2012; Harley 2017). An upper threshold of 2.5 m (H_U) was utilized to identify storms, representing the minimum requirement for H_s . Subsequently, a lower threshold of 1.5 m (H_L) was employed to identify the effective duration of the storm (Fig. 3). These two thresholds have been derived considering the long-term characteristics of the offshore wave climate at Hasaki (Nagai and Ogawa 2004).

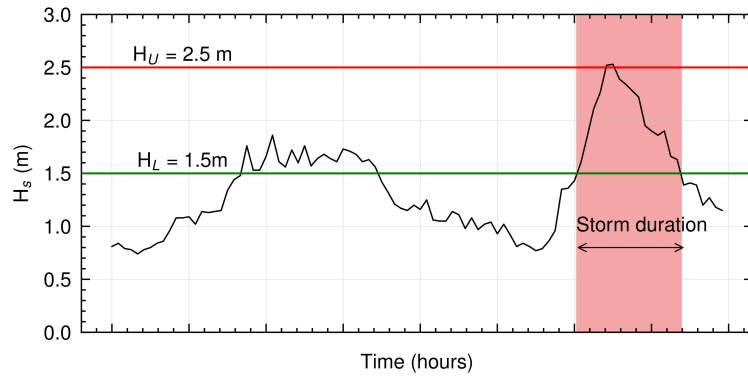


Figure 3. Storm identification based on a two-threshold (Upper limit: H_U , Lower limit: H_L) significant wave height approach.

3. Methodology

The flow chart of this research work is presented in Fig. 4. First, we tried to understand the feature importance of each indicator for different profile patterns for beach erosion. Then, the development of BESN was conducted considering the selected morphometric indicators, which significantly contributed to beach erosion.

3.1. Shoreline-based moving cross-shore profiling

HORS collects daily cross-sectional measurements in 5 m intervals ranging from -115 m to 385 m to assess the sediment exchange along the beach accurately. The Hasaki shoreline, in HORS coordinate system x, has varied from -36.9 m to 45.7 m during the study period (i.e. 1987-01 to 2010-12). Those variations are relative to the HORS native coordinate system, which has a fixed coordinate system relative to the pier's landside structure (a schematic illustrating this is available in Kuriyama (2002)). Recognizing the importance of shoreline position in crossshore sediment balance and longterm morphology changes, we made adjustments to the crossshore coordinate system. Thus each storm's shoreline in our coordinate system starts out at 0 (relative to HWL) with fixed cross-shore lengths (i.e. -80 m landward and 340 m offshore). The post-storm profile is then extracted from that same coordinate system assigned to a particular storm event (Fig. 6). This logic follows for all the storms considered in this study. This novel approach enabled us to focus on beach erosion and better

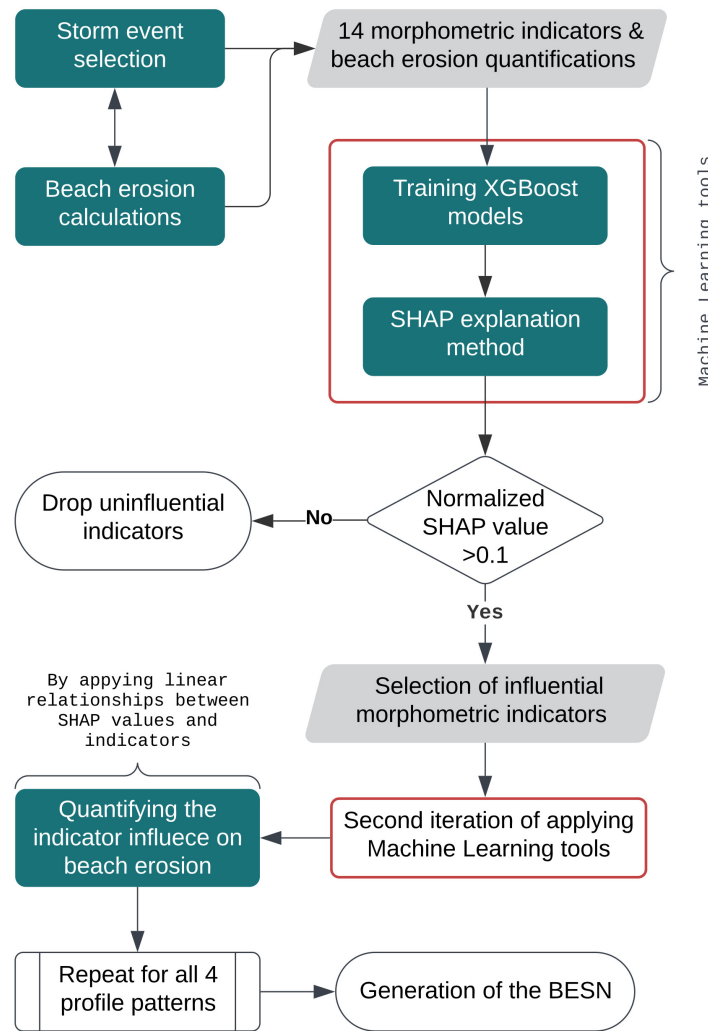


Figure 4. Flowchart of the BESN generation. The flowchart depicts the two-stage training process of the XGBoost models. In the second step of XGBoost training, the SHAP explanation methods are employed to generate the BESN, assuming a linear relationship between the selected indicators and SHAP values.

understand the vulnerability of the beach. Previous studies provided only a limited discussion of the impact of shoreline variation on beach vulnerability. (Alexandrakis and Poulos 2014; de Andrade, Sousa, and Siegle 2019). However, the pre-storm shoreline position significantly influenced the impact of storms on the beach (Thilakarathne et al. 2022), further emphasizing the importance of using a shoreline-based approach in beach profiling.

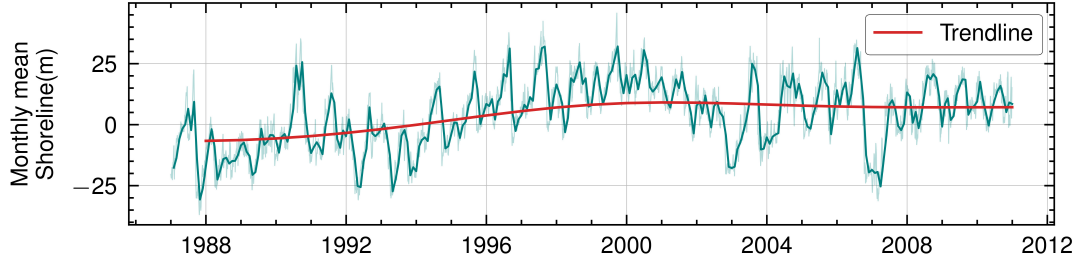


Figure 5. Monthly mean shoreline variation from 1987 to 2010. Weekly mean shoreline values are shown in light color, and the trendline based on the annual mean shoreline values is shown in red color.

The new shoreline-based 420 m moving cross-sectional zoning covers a section 80 m landward and 340 m seaward, as shown in Fig. 6. This profile section shifted landward and seaward based on the shoreline position. We could accurately examine wave action on the beach zone using these long-term data sets. Based on the closure depth at Hasaki, 20 m from the shoreline was selected as the beginning of the inner zone. In contrast, 170 m from the coastline was selected to separate the outer one from the inner zone considering the long-term sandbar formations.

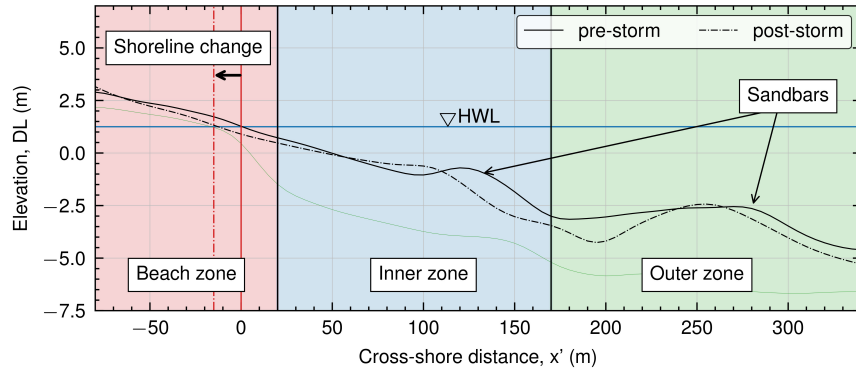


Figure 6. Profile definition based on shoreline position. The beach zone, the inner sandbar zone, and the outer sandbar zone are colored red, blue, and green, respectively. The black line represents the pre-storm profile, while the dotted line represents the post-storm profile. The red vertical line represents the pre-storm shoreline, while the dotted line represents the post-storm shoreline. Datum profile used for sediment volume quantification is shown in green line.

3.2. Profile patterning and sandbar morphometrics

Cross-shore sand movement on beaches with steeper slopes than the median slopes can cause temporal changes between the barred and unbarred profiles with a pronounced berm in the upper swash zone (Ruessink et al. 2016). Severe wave conditions during winter often lead to the erosion of beaches, causing the shoreline to shift landward.

Furthermore, eroded profiles are often accompanied by the formation of sandbars, which serve as underwater seawalls and assist in dissipating wave energy (Ciavola and Coco 2017). Whereas, accreted beaches have a more seaward shoreline during the summer, with fewer sandbars. Considering the impact of the presence of a sandbar on beach erosion, we have divided the beach profiles into four main categories and investigated their respective roles in beach erosion susceptibility.

In a recent study, Januait et al. (2021) discussed the realignment of nearshore sandbars and their impact on nearshore changes and sub-aerial beaches. They highlighted the role of sandbar switching location, sandbar cross-shore location, shoreline positions, and sand volume changes in beach erosion. Although our analysis focused on storm-related time scales, their findings on long-term morphology changes remain relevant. Therefore, understanding the location of sandbars is crucial in predicting beach shape and wave energy distribution, enabling effective planning for coastal erosion, beach nourishment, recreational activities, and other coastal management strategies.

A Python signal processing toolbox known as the Gaussian 1d filtering library, available in the SciPy package (Virtanen et al. 2020), was utilized to process the daily cross-shore survey data. This toolbox was employed to smooth the beach profiles and identify the crests and troughs of the sandbars (Fig. 7). To exclude insignificant sandbar formations, a minimum height threshold of 0.24 m was used for inner zone sandbars and 0.5 m for outer zone sandbars considering the long-term sandbar characteristics at Hasaki. The sandbar features considered in this study include the distance from the shoreline to the sandbar crest, the sandbar depth based on the water depth relative to the high water level (HWL) at Hasaki (1.252 m), and the slopes of the sandbars in the seaward and landward directions.

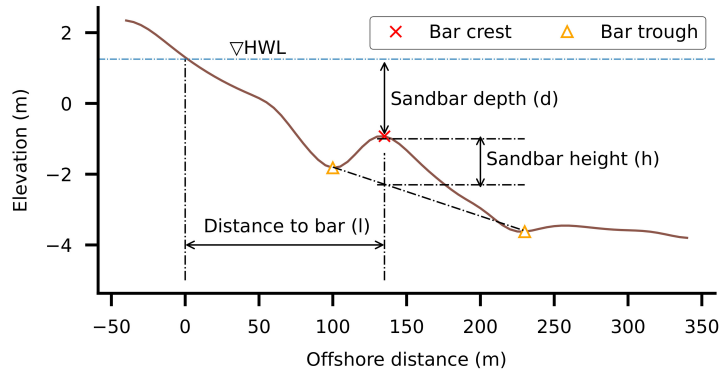


Figure 7. Quantifying sandbar features as morphometric indicators for susceptibility analysis.

Based on the presence and location of sandbar crests, the beach profiles were classified into four patterns: unbarred profiles, inner zone sandbar profiles, outer zone sandbar profiles, and double sandbar profiles (Fig. 8). The objective was to identify the distinct characteristics of each profile type that contribute to beach susceptibility. Furthermore, the presence of sandbar formations indicated different phases of long-term sandbar migration, and this patterning of profiles could potentially aid in identifying such phases.

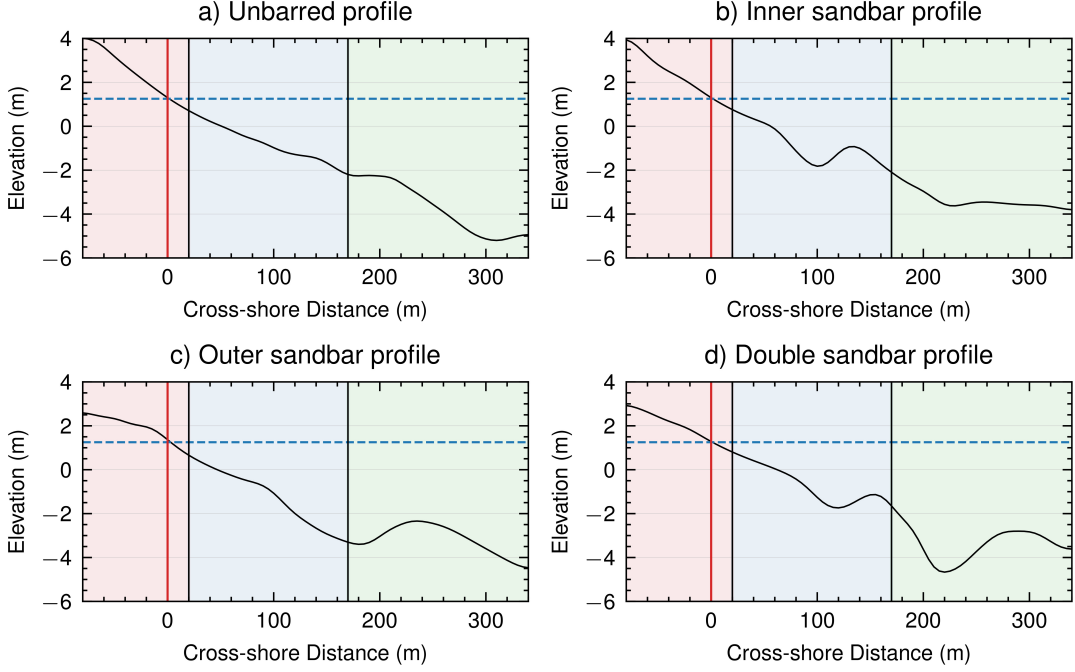


Figure 8. Main beach profile patterns: a) unbarred profiles, b) inner sandbar profiles, c) outer sandbar profiles, and d) multiple sandbar profiles.

3.3. Morphometric indicators

Table 1 summarizes all the morphometric indicators examined in the statistical analysis. These indicators were carefully selected to represent the profile characteristics ranging from the backshore area to the offshore sandbar formations. Given the study's specific focus on the impact of sandbar formations, five sandbar features were considered (Fig. 7). The key morphometrics for each profile pattern were identified by assessing the contribution of each indicator to beach erosion. Subsequently, the beach susceptibility was quantified based on the respective contributions of the selected features to volumetric beach erosion.

3.4. XGBoost regression model

XGBoost models were trained with three hyperparameters, namely *n_estimators*, *max_depth*, and *learning_rate* (Chen and Guestrin 2016). The *n_estimators* parameter defines the number of decision trees to be used in the model, which was set to 1000 in this study. Increasing this parameter could improve the performance but at the expense of longer training times. The *max_depth* parameter was set to 10 in this study, specifying the maximum depth of each decision tree. This parameter affects the complexity of each decision tree and controls the level of overfitting in the model. A higher value of *max_depth* could lead to more complex trees and increase the risk of overfitting. Finally, the *learning_rate* parameter was set to 0.1 in this study, which sets the step size at each iteration of the boosting process. This parameter impacts the convergence rate and update size at each step.

Table 1. Morphometric indicators (indicators) used in this analysis to quantify the beach profile susceptibility.

Notation	indicator	Description
A	Shoreline position [m]	Shoreline of the previous day's beach profile
B	Inner zone sediment volume [$m^3 m^{-1}$]	Volumetric sediment deposition in the inner zone relative to the datum profile, which is based on the lowest cross-section elevation measurements
C	Outer zone sediment volume [$m^3 m^{-1}$]	Volumetric sediment deposition in the outer zone relative to the datum profile, which is based on the lowest cross-section elevation measurements
D	Beach slope	Tangential beach slope of foreshore (vertical height/100 m)
E	Inner sandbar height [m]	
F	Inner sandbar distance [m]	
G	Inner sandbar water depth [m]	Sandbar formations in the inner zone (20 m to 170 m) are characterized based on Fig. 6
H	Inner sandbar landward slope	
I	Inner sandbar landward slope	
J	Outer sandbar height [m]	
K	Outer sandbar distance [m]	
L	Outer sandbar water depth [m]	Sandbar formations in the outer zone (170 m to 340 m) are characterized based on Fig. 6
M	Outer sandbar landward slope	
N	Outer sandbar landward slope	

3.5. SHAP explanation method

SHAP (SHapley Additive exPlanations) is a widely recognized technique that utilizes the concept of Shapley values from cooperative game theory to explain complex machine learning models (Lundberg and Lee 2017). This technique quantifies the contribution of each feature in a prediction by assessing the marginal contributions of individual features to the model output. This is achieved by comparing the model's predictions when the complete feature set is used to the predictions obtained when each feature is removed. These marginal contributions are then aggregated using a weighted sum, resulting in the computation of the Shapley value for each feature. The weighting scheme considers the number of possible feature combinations that include or exclude the evaluated feature. SHAP can provide both global and local explanations for individual predictions by calculating Shapley values for each feature across multiple predictions. The Shapley value equation is employed to determine the marginal contribution of each feature to the model output (Eq. 1).

$$\Phi_i = \frac{1}{M!} \sum_R [E[f(x)|x_{S_i^R \cup \{i\}}] - E[f(x)|x_{S_i^R}]] \quad (1)$$

In this equation, Φ_i represents the Shapley value for feature i . The term $E[f(x)|x_{S_i^R \cup i}]$ represents the expected model output, for instance, R , when feature i is included, while $E[f(x)|x_{S_i^R}]$ represents the expected model output, for instance, R , when feature i is excluded. Additionally, M corresponds to the total number of possible feature combinations (coalitions).

3.6. Generation of Beach Erosion Susceptibility Number, BESN

After identifying the key indicators using XGBoost and SHAP explanation methods, the selected indicators are utilized to quantify the susceptibility characteristic of the beach profile by considering their magnitude and significance in relation to beach

erosion. Each morphometric indicator is denoted as I . The steps involved in generating the BESN are outlined below.

Step 1: Indicator Normalization

Normalization was applied to each indicator to ensure the generalizability of the BESN and disregard the original value ranges. This was particularly important as the value ranges of the indicators can vary significantly. For example, the shoreline indicator might range from -36.9 m to 45.7 m in the HORS coordinate system, x , while the inner sandbar height indicator might range from 0.2 m to 2.3 m. To achieve normalization, the indicator values were transformed using Equation 2.

$$I_{\text{norm}} = \frac{I - I_{\min}}{I_{\max} - I_{\min}} \quad (2)$$

Step 2: Weights for BESN

Weights were assigned to each normalized indicator to account for their varying contributions to beach erosion and, consequently, beach susceptibility. The weights (w_i) were determined based on the SHAP values, which quantify the impact of each indicator on beach susceptibility. Equation 3 was used to ensure that the weights add up to one and maintain their relative proportions.

$$\bar{w}_i = \frac{w_i}{\sum_i w_i} \quad (3)$$

Step 3: Linear functions for weights

A linear function was introduced to capture the relationships between SHAP values and indicator weights more accurately. This was necessary due to the observed variation in SHAP values for different indicator values, which also affected the corresponding weights. We could better account for the complex relationships between indicators and beach susceptibility by calculating coefficients c_f and m for each selected indicator within each profile pattern, leveraging the local interpretability of SHAP values (Eq. 4).

$$\bar{w}_i = c_f I_i + m \quad (4)$$

Step 4: Discretization of BESN generations

In the final step of the BESN generation process, the continuous BESN data obtained by multiplying the corresponding I_i values with Eq. 4 were discretized into five separate data bins using NumPy (Eq.5)(Harris et al. 2020). This discretization enabled us to categorize the beach profiles effectively according to their susceptibility to erosion. Higher BESN values indicated a greater vulnerability to erosion, while lower values suggested a lower susceptibility.

$$\text{BESN} = \text{discretize} \left(\sum (c_f I_i + m) I_i \right) \quad (5)$$

4. Analysis of key morphometric indicators on beach erosion

This section presents the results and discussion of the SHAP value calculation and the contribution of morphometric indicators and selection in generating BESN. Our storm identification method detected 347 storm events from 1987 to 2010 at Hasaki. A summary of the statistical analysis of the 14 morphometric indicators for each pre-storm beach profile is listed in Table 2.

Table 2. Indicator description and statistical summary of all the 14 morphometric indicators.

ID	Morphometric indicator	Mean	St. d	Min	Max
A	Shoreline [m]	2.67	12.97	-27.93	39.09
B	Inner zone volume [$\text{m}^3 \text{ m}^{-1}$]	383.0	76.0	70.7	489.1
C	Outer zone volume [$\text{m}^3 \text{ m}^{-1}$]	432.5	83.4	183.5	607.4
D	Beach slope	0.031	0.024	0.010	0.133
E	Inner zone sandbar Height [m]	0.90	0.48	0.25	2.32
F	Inner zone sandbar distance [m]	132.15	27.59	55.00	170.00
G	Inner zone sandbar depth [m]	2.31	0.65	1.04	4.10
H	Inner zone sandbar slope landward	0.011	0.0083	0.000	0.040
I	Inner zone sandbar slope seaward	0.031	0.009	0.012	0.061
J	Outer zone sandbar height [m]	1.32	0.51	0.50	2.67
K	Outer zone sandbar distance [m]	245.65	48.86	175.00	335.00
L	Outer zone sandbar depth [m]	3.63	0.75	2.23	6.54
M	Outer zone sandbar slope landward	0.018	0.009	0.002	0.048
N	Outer zone sandbar slope seaward	0.022	0.011	0.000	0.047

4.1. Feature importance analysis

We used four distinct XGBoost regression models with the complete data set of storm events for each profile pattern to quantify the susceptibility of each profile type (Table 3). To capture the contribution of each morphometric, we utilized all the storm data in each profile pattern to train all four XGBoost models. A validation phase was not conducted because the purpose of using these boosting tree models was simply to understand the complex interactions between morphometrics and beach susceptibility through the SHAP explanation method.

Table 3. Number of beach erosion cases in each pattern.

Profile shape ^a	Number of profiles
Unbarred profiles	40
Inner sandbar profiles	92
Outer sandbar profiles	130
Double sandbar profiles	85

^a Beach profile separation based on the sandbar presence and formation is described in Chapter 3.2.

SHAP values were extracted for each storm case in each profile pattern, resulting in a set of values quantifying the contribution of each morphometric in each event. A positive SHAP value (+) indicated a contribution to beach erosion, while a negative value (−) indicated the opposite effect. Mean absolute values for each morphometric were calculated in each profile pattern to identify key morphometrics. These SHAP values, referred to as weights in the BESN generation, were normalized by dividing their sum. A threshold of 0.1 was applied to separate the most significant morphometrics in each

profile pattern.

4.2. Linear weight functions for each profile pattern

The generated linear functions for each indicator in each profile pattern shown in Eq. 4 are discussed in four separate subsections. Each subsection focuses on the role of each morphometric in different profile patterns and provides insights based on the corresponding SHAP values. The analysis explores the impact of these indicators on beach susceptibility. However, it is important to acknowledge that fitting morphometric indicators and SHAP values to linear functions may not fully capture the complexity of these relationships. While linearity simplifies the relations, it aids in providing a more direct understanding of their impact on beach susceptibility.

4.2.1. Unbarred profiles

Fig. 9 shows the distribution of SHAP values for each indicator in the presence of unbarred profiles. As shown in Fig.9a and Fig.9b, the initial shoreline (A) and inner-zone sediment volume (B) are the most influential indicators contributing to erosion susceptibility. Therefore, these indicators are identified as significant contributors to beach susceptibility. Fig.9c clearly demonstrates the positive and negative influences of shoreline position on beach susceptibility. Although the linearity between SHAP values and inner-zone sediment volume is unclear, Fig.9d shows relatively larger SHAP values, indicating the significant influence of inner-zone sediment volume on beach susceptibility.

The inner-zone sediment volume is the primary indicator influencing beach erosion, and it exhibits a negative correlation. However, Fig. 9d reveals that the SHAP values demonstrate a positive correlation when the inner-zone sediment volumes exceed 0.9. Interestingly, we also observed that the relationship between erosion susceptibility and inner-zone sediment volume depends on the initial condition of the beach profile. Specifically, already eroded inner-zone profiles were more prone to erosion than uneroded profiles with the same sediment volume. This highlighted the importance of considering the initial condition of the beach profile in erosion vulnerability assessments. However, the slope of the beach profile was found to have no significant impact on erosion susceptibility, implying that other factors may be more effective in erosion mitigation efforts for unbarred profiles. Additionally, the impact of outer-zone sediment volume on erosion susceptibility was negligible.

4.2.2. Inner sandbar profiles

Fig. 10 shows an overview of the distribution of SHAP values for each indicator in inner sandbar profiles. Fig.10a and Fig.10b reveal that the initial shoreline (A), fore-shore slope (D), inner sandbar height (E), and inner-sandbar seaward slope (I) are the most influential indicators contributing to erosion susceptibility. However, the impact of indicators A and I on erosion susceptibility is unclear, as indicated by the scattered data points observed in Fig.10c and Fig.10f. Conversely, indicator D exhibits higher SHAP values, suggesting its significance in influencing the erosion susceptibility of beach profiles. Additionally, while the linearity between SHAP values and inner sandbar height is not clearly shown, Fig.10e consistently demonstrates negative SHAP values.

The presence of an inner sandbar reduces beach erosion and, subsequently, beach

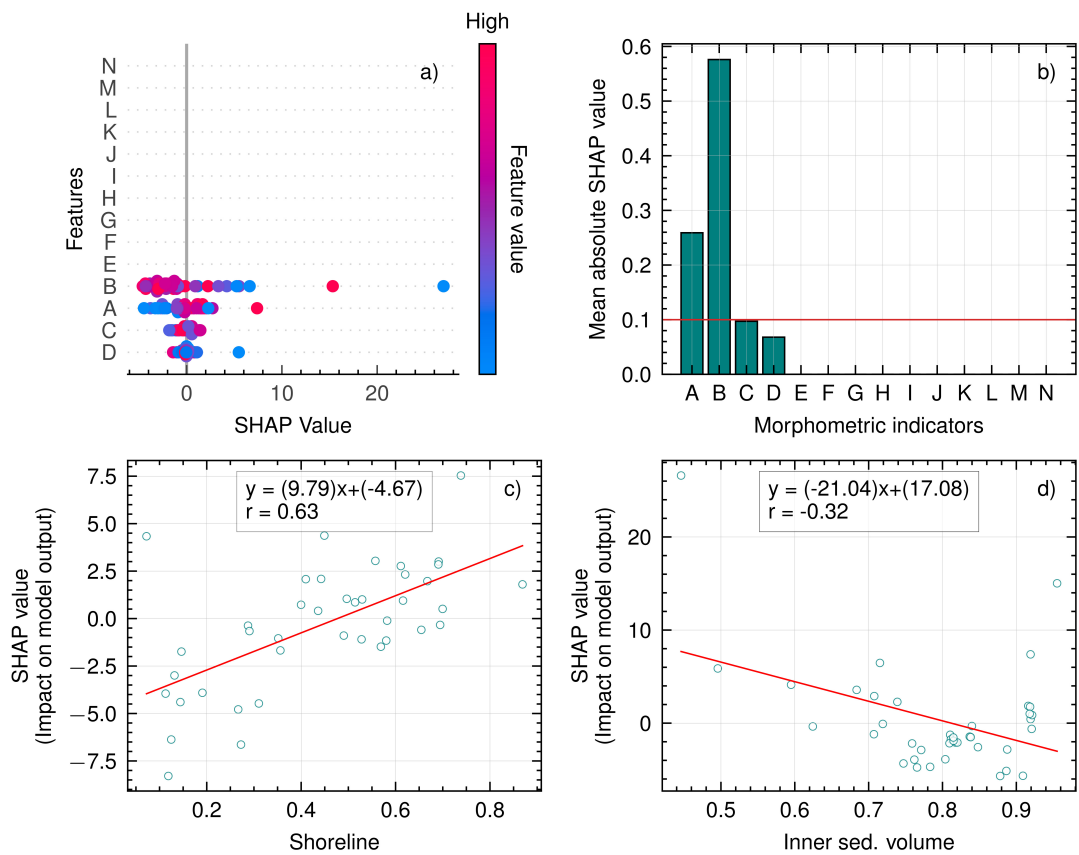


Figure 9. SHAP value variation with each morphometric for unbarred profile patterns: a) SHAP summary plot, b) bar plot of mean absolute SHAP values, c) correlation between SHAP values and normalized initial shoreline, d) correlation between SHAP values and normalized inner zone sediment volumes.

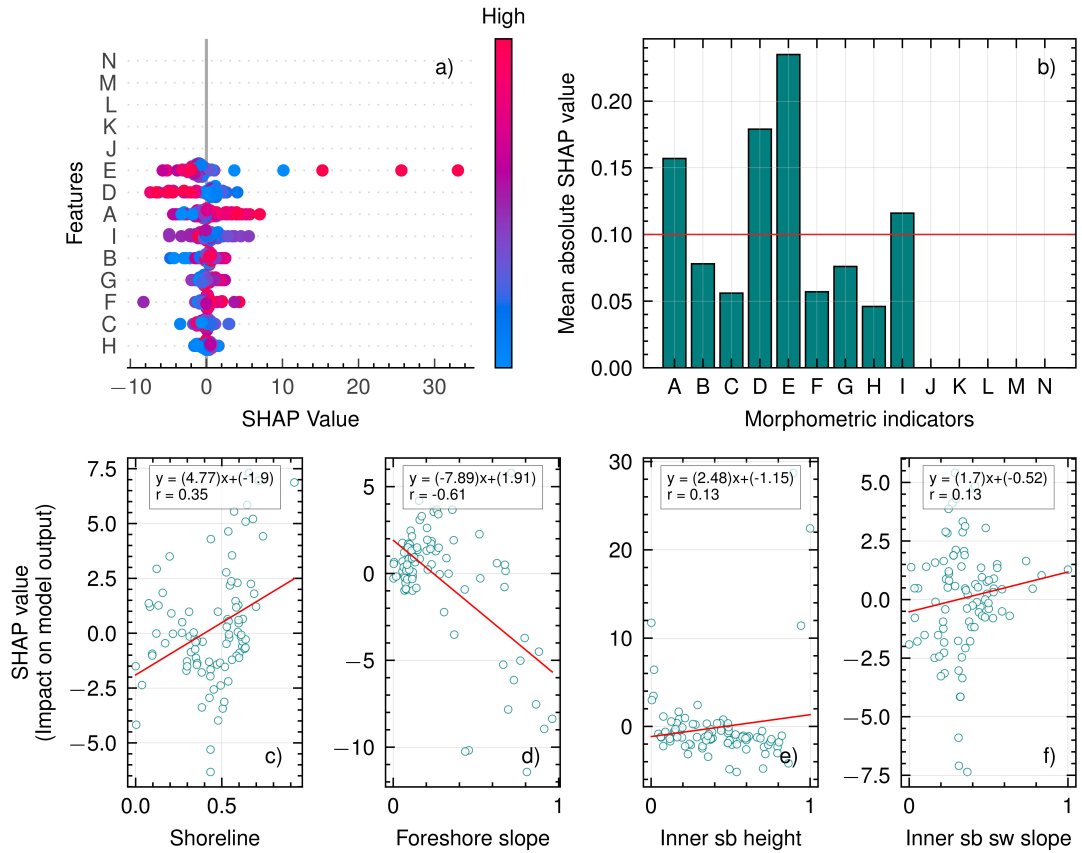


Figure 10. Variation of SHAP values with each morphometric for inner sandbar profile patterns: a) SHAP summary plot; b) bar plot of mean absolute SHAP values; c) correlation between SHAP values and initial shoreline; d) correlation between SHAP values and foreshore slope; e) correlation between SHAP values and inner sandbar height; f) correlation between SHAP values and inner sandbar seaward slope.

susceptibility. This observation aligns with the hypothesis that inner sandbar formation has a beneficial impact on reducing beach erosion. However, when milder seaward slopes are present, the influence of the indicator becomes less clear, as indicated by the scattered positive and negative SHAP values in Fig.10f. This finding is supported by Bujan, Cox, and Masselink (2019), who showed that gentle slopes encourage beach erosion, resulting in highly susceptible and fragile beach profiles. Notably, the majority of SHAP values for indicator E display a consistent negative pattern, suggesting its contribution to reducing beach susceptibility. Moreover, the higher outer-zone sediment volumes are not necessarily significant, as their contribution is negligible, as shown in Fig. 10b. Furthermore, the location and depth of the inner sandbar have no significant influence on beach susceptibility.

4.2.3. Outer sandbar profiles

Fig. 11 shows an overview of the distribution of SHAP values for each indicator in outer sandbar profiles. Fig.11a and Fig.11b reveal that the initial shoreline (A), inner-zone sediment volume (B), outer-zone sediment volume (C), and outer sandbar depth (L) are the most influential indicators contributing to erosion susceptibility in outer sandbar profiles. The initial shoreline position shows a good linear fit, indicating its importance in quantifying beach susceptibility for this profile pattern. Sandbar depth has the most significant influence on erosion susceptibility among the other outer sandbar characteristics, as evidenced by its significant mean SHAP value. Although both indicators B and C have an impact, the impact of B, inner-zone sediment volume, is significantly greater.

Fig.11c illustrates that eroded beaches, i.e., landward shorelines, result in low susceptibility beach profiles, whereas higher seaward shorelines increase susceptibility. The staggered higher indicator values of B indicate its importance in quantifying susceptibility, as reflected by the higher SHAP values in Fig.11d. Although indicator C is less influential, it is a good fit for a linear function used in BESN calculations. A satisfactory linear fit is crucial for a better BESN quantification. Additionally, indicator L demonstrates a good linear fit to the data in Fig.11f. However, lower outer sandbar depths help to reduce erosion susceptibility. This is primarily because lower water depths cause wave breaking before reaching the beach, resulting in lower wave energy reaching the beach and reduced erosion susceptibility.

4.2.4. Double sandbar profiles

Fig. 12 shows an overview of the distribution of SHAP values for each indicator in double sandbar profiles. Fig.12a and Fig.12b reveal that the initial shoreline (A) and outer-zone sediment volume (C) are the most influential indicators contributing to erosion susceptibility in double sandbar profiles. These selected indicators exhibit a good linear fit, indicating their importance in quantifying beach susceptibility for this profile pattern. Both indicators A and C demonstrate the influence on erosion susceptibility, as they exhibit relatively higher mean absolute SHAP values than the other 12 indicators.

Although 14 morphometric indicators were tested, using the same threshold of 0.1 for significant indicator selection may not be appropriate. However, the selected indicators and the other 12 indicators clearly showed mean SHAP value differences (Fig.12b), indicating their relative importance. Specifically, advanced shoreline positions, i.e., seaward shorelines, were associated with increased susceptibility to erosion,

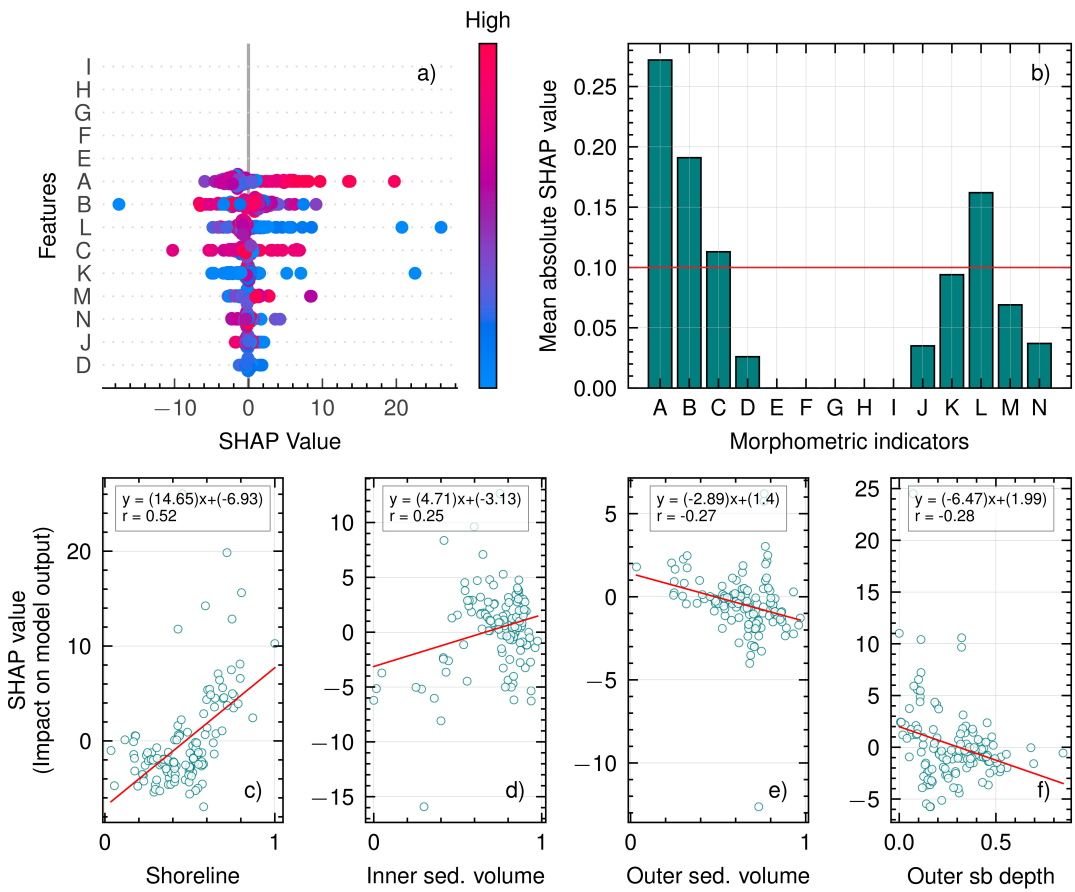


Figure 11. Variation of SHAP values with each morphometric for outer sandbar profile patterns: a) SHAP summary plot; b) bar plot of mean absolute SHAP values; c) correlation between SHAP values and normalized initial shoreline; d) correlation between SHAP values and normalized inner zone sediment volumes; e) correlation between SHAP values and normalized outer zone sediment volumes; f) correlation between SHAP values and normalized outer sandbar depth.

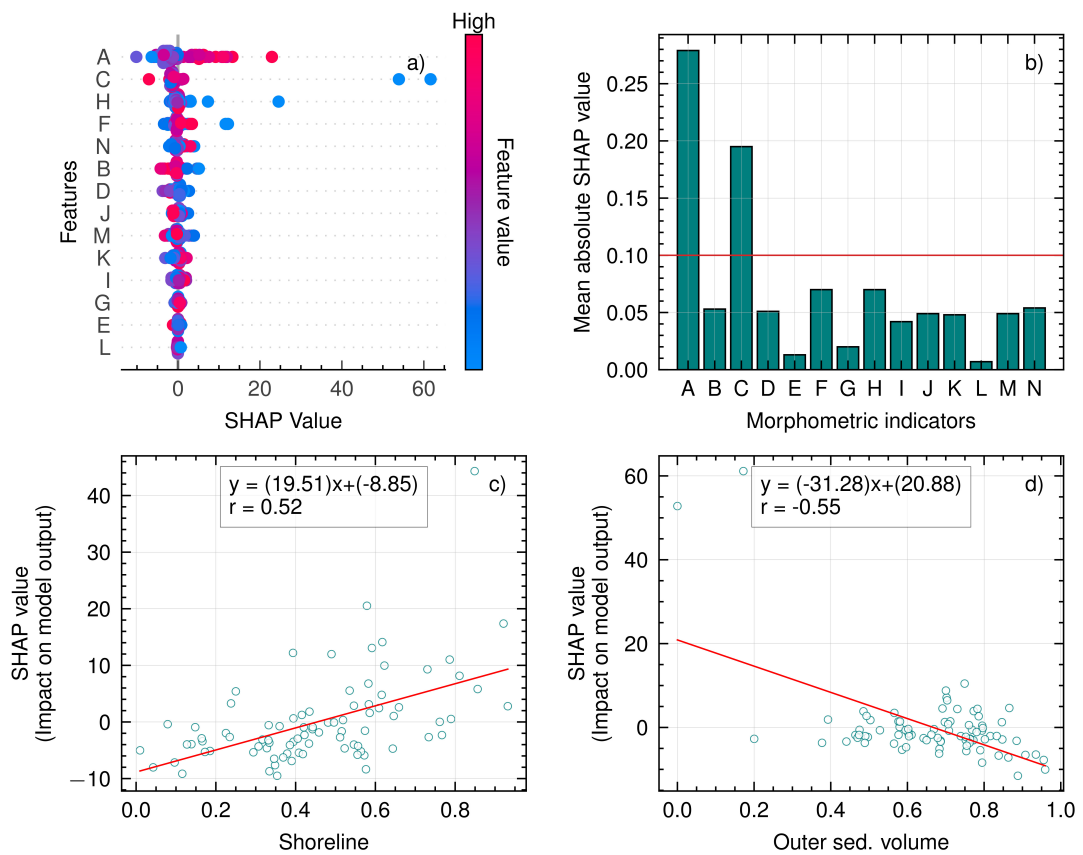


Figure 12. SHAP value variation with each morphometric for double sandbar profile patterns: a) SHAP summary plot; b) bar plot of mean absolute SHAP values; c) correlation between SHAP values and Initial shoreline; d) correlation between SHAP values and outer zone sediment volume.

as indicated by the finer distribution of SHAP values in Fig.12c. This behavior was consistent with the findings observed in other profile patterns. However, the impact of outer-zone sediment volume (C) was predominantly negative, indicating its significance in reducing the susceptibility of the beach to storm-induced erosion, as shown in Fig.12d.

The formation of double sandbar profiles is generally considered the final phase of long-term sandbar migration in winter profiles (Vidal-Ruiz and Ruiz de Alegria-Arzaburu 2019). However, understanding the comprehensive physical mechanisms related to all 14 morphometric indicators in the context of sediment exchange is complex. Nevertheless, this study highlights the importance of carefully considering the effects of shoreline position and outer-zone sediment volume when designing coastal protection measures for double sandbar profiles.

5. Beach Erosion Susceptibility Number

Table 4 summarizes the most influential indicators in each profile pattern based on the 0.1 thresholds. The relationships between the SHAP values and morphometric indicators are illustrated in Fig. 9 to 12 (Chapter 4). Based on these relationships, linear functions for the weights were derived using Eq. 4. The resulting weight functions are presented in Table5. Subsequently, the BESN values were calculated by applying the weight functions to the normalized indicators (Eq. 5).

Table 4. Selecting the most influential morphometric indicators for each of the profile patterns.

Profile shape	Number of profiles	Influential morphometric Indicator
Unbarred profiles	40	Shoreline, Inner zone volume, Outer zone volume
Inner sandbar profiles	92	Inner zone volume, Foreshore slope, Inner sandbar height
Outer sandbar profiles	130	Inner zone volume, Outer zone volume, Foreshore slope, Outer sandbar depth
Double sandbar profiles	85	Shoreline, Outer zone volume

Table 5. Gradients (m) and coefficients (c_f) of weight functions for each morphometric indicator for different profile patterns.

Profile type	Weight function	Morphometric values						
		A	B	C	D	E	I	L
Unbarred	m	9.97	-21.04	-	-	-	-	-
	c_f	-4.67	17.08	-	-	-	-	-
Inner sandbar	m	4.77	-	-	-7.89	2.48	1.70	-
	c_f	-1.90	-	-	1.91	-1.15	-0.52	-
Outer sandbar	m	14.65	4.71	-2.89	-	-	-	-6.47
	c_f	6.93	-3.13	1.40	-	-	-	1.99
Double sandbar	m	19.51	-	-31.28	-	-	-	-
	c_f	-8.85	-	20.88	-	-	-	-

5.1. Performance of Beach Erosion Susceptibility Number

Actual measurements of beach erosion are compared to the corresponding BESN values to determine the accuracy of BESN predictions. Higher BESN values indicate a higher susceptibility of beach profiles to erosion, implying a higher probability of significant erosion. However, it is important to note that beach erosion is also influenced by wave energy conditions during a storm event. The storm power (P) is calculated using the maximum significant wave height ($H_{s\text{-max}}$) recorded during the storm duration (D) in hours to quantify the wave energy condition. The storm power (P) can be calculated using the following equation:

$$\text{Storm Power} = H_{s\text{-max}}^2 \times D \quad (6)$$

The 347 observed erosion events were divided into three categories based on their storm power values: mild, average, and severe storm conditions. The thresholds of $500 \text{ m}^2 \text{ h}$ and $1000 \text{ m}^2 \text{ h}$ were used to classify the erosion events into these categories, as shown in Fig. 13. This categorization enabled for a comprehensive evaluation of BESN performance under different storm power conditions, providing insights into its effectiveness in capturing the susceptibility of beach profiles to erosion.

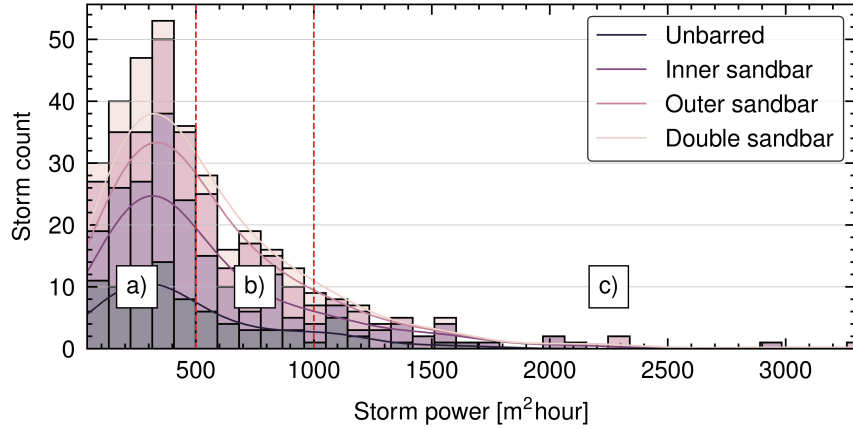


Figure 13. Storm power histogram was used to divide the complete data set into three groups for BESN validation based on storm power [$\text{m}^2 \text{ h}$]: a) mild storm conditions, b) average storm conditions, and c) severe storm conditions. The red vertical dotted lines indicate the boundaries separating the groups.

It was assumed that grouping erosion events based on similar storm conditions would result in a consistent impact on erosion by wave conditions. The performance of BESN for three different storm conditions is illustrated in Fig. 14. Table 6 summarizes the statistical performance of BESN for each profile pattern and storm condition based on the Pearson correlation coefficient (r). Moderate correlations were observed for inner, double, and outer sandbar profiles during severe storm conditions. However, unbarred profiles showed minimal correlation. Both unbarred and outer sandbar profile patterns displayed significant correlations under mild storm conditions, which encompassed many storm cases. In the case of average storm conditions, unbarred profiles exhibited a strong correlation coefficient of 0.75. Inner and outer sandbar profiles also demonstrated good performance, while the correlation for double sandbar profiles was relatively weaker. Although some BESN predictions did not fully satisfy expectations, most cases indicated a positive relationship between BESN values and observed erosion.

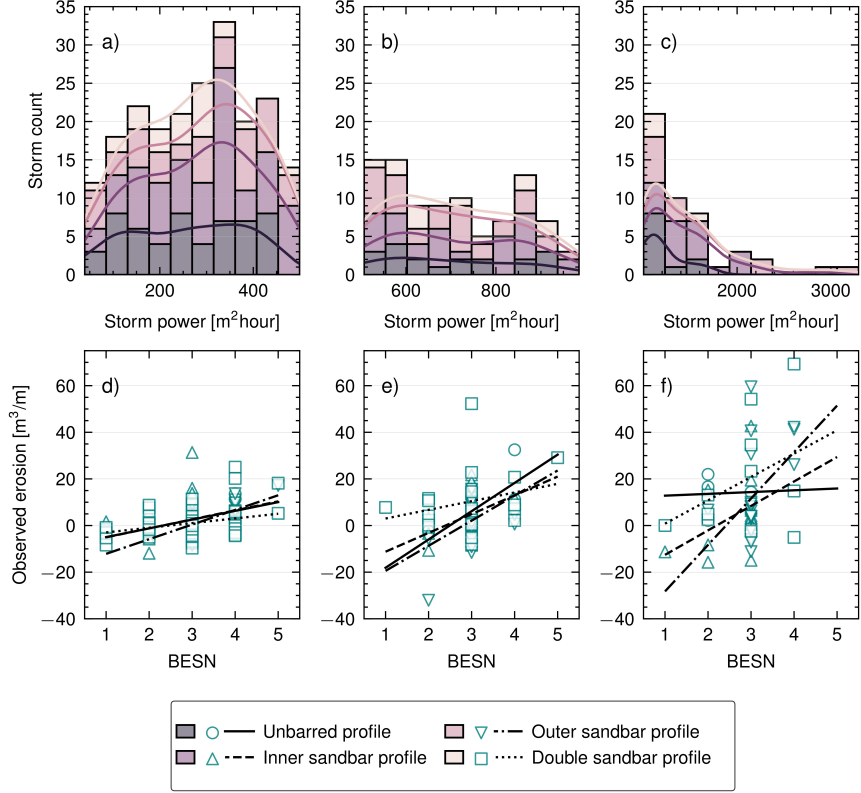


Figure 14. BESN Validation for different storm conditions: Storms are categorized into three groups based on storm power thresholds of $500 \text{ m}^2 \text{ h}$ and $1000 \text{ m}^2 \text{ h}$. Panels (a-c) display the distribution of storms across the storm power groups, with different profile patterns represented by different colors. Panels (d-f) illustrate the correlation between eroded volume and BESN, where distinct markers and lines depict each of the four profile patterns.

Table 6. Performance of the BESN for different profile types and storm conditions. The Pearson correlation coefficient (r) values between BESN and observed beach erosion are utilized as a measure of the performance of BESN. The corresponding significance levels of the correlation coefficients are indicated in parentheses.

Profile type	Pearson r values (significance)		
	Mild storms	Average storms	Severe storms
Unbarred	0.53 (0.01)	0.75 (0.01)	0.05 (0.95)
Inner sandbar	0.22 (0.13)	0.40 (0.02)	0.42 (0.24)
Outer sandbar	0.54 (0.00)	0.40 (0.03)	0.46 (0.04)
Double sandbar	0.31 (0.02)	0.26 (0.28)	0.40 (0.22)

5.2. Applicability of the BESN

The BESN was introduced to quantify the beach susceptibility, also referred to as fragility or sensitivity in other studies, of different beach profile patterns. The BESN was designed to act as an indicator of a beach profile's susceptibility to erosion. Our observations at Hasaki indicated that morphological characteristics such as sandbar formations also influence beach susceptibility. Most of the previous coastal vulnerability studies have overlooked the importance of considering beach-specific vulnerability indicators in their research (Gornitz, White, and Cushman 1991; Denner et al. 2015; Doukakis 2005; Koroglu et al. 2019). Although long-term changes in beach morphology, such as sandbar migration, are often seasonal, our focus in the development of BESN was on a storm-wise susceptibility quantification approach rather than long-term changes.

The Pearson correlation coefficient (r) was initially used to assess the relationship between the selected 14 morphometric indicators and beach susceptibility. However, it was acknowledged that relying solely on Pearson r has limitations because it provides only a single value to represent the relationship between an indicator and beach erosion. This approach did not consider the specific contribution of each indicator, which can vary in importance. The SHAP explanation method was employed to address this limitation, which offers both local and global interpretability for the models. The SHAP values provided insights into the contribution of each indicator on a local level, allowing for a more comprehensive understanding of their significance in predicting beach erosion. When combined with theoretical knowledge, the SHAP findings helped to validate the findings and ensure the robustness of the approach.

Although the seasonality factor was not explicitly considered in this study, it is recognized that seasonal variations, particularly during winter, play a crucial role in severe erosion events and the formation of sandbars with mild slopes in the outer zone. The presence of sandbars and milder slopes could impact beach profile susceptibility. Although three groups were defined based on different wave conditions in this study, it is recommended to further validate the approach through numerical simulations under consistent wave conditions in future work. This would provide a more comprehensive validation of the proposed methodology and enhance the accuracy of beach profile susceptibility quantification.

The importance of maintaining natural sediment balance in a coastal system, particularly in the face of human disturbances, has led to the popularity of relatively low-cost beach nourishment efforts. To optimize these efforts, a holistic approach is required to assess the susceptibility of a beach profile to erosion. In this regard, the proposed BESN effectively identifies the most susceptible areas and aid to conduct nourishment accordingly. Long-term analysis of beach susceptibility also enables coastal stakeholders to make informed decisions regarding the need for shore protection action. Although several previous studies on beach nourishment have focused on dunes, sandbar formations have been relatively understudied due to a lack of data (Greene 2002; Hanson et al. 2002; Elko et al. 2021). Our study provides valuable insights into the impact of sandbars on beach susceptibility, which can guide future research in this area and help justify the omission of certain indicators. Furthermore, BESN can also be used to determine the optimal timing for soft protection measures such as nourishment. Artificial nourishment has been shown to have minimal negative impact compared to other shore protection options. The use of BESN to identify vulnerable locations along a coastline allows for the effective execution of necessary shore protection actions.

6. Conclusion

The impact of morphometric indicators on beach erosion susceptibility is closely related to the shape of the beach profile and the position of the shoreline. The analysis revealed that different profile patterns play a significant role in determining the indicators contributing to beach erosion. For example, the inner zone sediment volume was a critical factor only in the presence of unbarred and double sandbar profiles. The height of the inner zone sandbar contributed to erosion susceptibility, but its influence diminished when double sandbars were present. The susceptibility of the beach to erosion was also influenced by sediment deposition in both the inner and outer zones, which can have either negative or positive effects depending on the magnitude of the sediment volume and the profile pattern. Furthermore, the foreshore beach slopes emerged as primary morphometric indicators that govern beach susceptibility when inner sandbars were present. These conclusions were based on the statistical analysis of morphometric indicator selection.

The study found the BESN quantification to be satisfactory. However, it was observed that different wave conditions significantly impact the BESN quantification. To further validate the performance of the proposed BESN, the authors propose conducting controlled numerical and physical modeling experiments under similar hydrodynamic conditions, as previously discussed. Additionally, because the study used data from a single location, testing the approach in other locations is required to determine its applicability. Although susceptibility approaches are typically site-specific and indicator-dependent, similar morphometric conditions of sandy beaches should be considered when adapting the approach to other locations. The proposed method can be applied to different locations with advancements in data availability. The separation of profile patterns has proved valuable in accurately quantifying beach susceptibility.

The study has some limitations and suggestions for future research. One limitation is the lack of similar wave conditions, and the applicability of the study is limited to sandy beaches. We strongly recommend the incorporation of additional beach profiles with similar morphology characteristics into our model. Making use of open datasets available worldwide such as Turner et al. (2016) can significantly enhance the results of the present study. Future work should focus on quantifying beach recovery potential. The authors intend to propose a comprehensive beach vulnerability index approach by combining susceptibility and recovery potential. Additionally, the study suggests the possibility of developing a real-time vulnerability prediction approach for economically and ecologically important beach locations.

Acknowledgments

We admiringly acknowledge the support extended by PARI, especially the Coastal and Estuarine Sediment Dynamic group led by Dr. Masayuki Banno, during the data collection stage of the present study. We are also grateful for the valuable comments provided by Dr. Hiroto Higa during the methodology development of this study. We extend our heartfelt thanks to the anonymous reviewers for their invaluable feedback and support during the revision process. Their input significantly enhanced the quality of this article.

Disclosure statement

No potential conflict of interest was reported by the author(s).

References

- Alexandrakis, George, and Serafim Poulos. 2014. "An holistic approach to beach erosion vulnerability assessment." *Scientific Reports* 4 (1): 6078. Number: 1 Publisher: Nature Publishing Group, <https://doi.org/10.1038/srep06078>, Accessed 2023-05-10. <https://www.nature.com/articles/srep06078>.
- Banno, Masayuki, Satoshi Nakamura, Taichi Kosako, Yasuyuki Nakagawa, Shin-ichi Yanagishima, and Yoshiaki Kuriyama. 2020. "Long-Term Observations of Beach Variability at Hasaki, Japan." *Journal of Marine Science and Engineering* 8 (11): 871. Number: 11 Publisher: Multidisciplinary Digital Publishing Institute, <https://doi.org/10.3390/jmse8110871>, Accessed 2023-07-10. <https://www.mdpi.com/2077-1312/8/11/871>.
- Basco, David R., and Nader Mahmoudpour. 2012. "The Modified Coastal Storm Impulse (COSI) Parameter and Quantification of Fragility Curves for Coastal Design." *Coastal Engineering Proceedings* (33): 66–66. Number: 33, <https://doi.org/10.9753/icce.v33.management.66>.
- Bujan, Nans, Rhadh Cox, and Gerd Masselink. 2019. "From fine sand to boulders: Examining the relationship between beach-face slope and sediment size." *Marine Geology* 417: 106012. <https://doi.org/10.1016/j.margeo.2019.106012>, Accessed 2023-05-15. <https://www.sciencedirect.com/science/article/pii/S0025322718304365>.
- Callaghan, D. P., P. Nielsen, A. Short, and R. Ranasinghe. 2008. "Statistical simulation of wave climate and extreme beach erosion." *Coastal Engineering* 55 (5): 375–390. <https://doi.org/10.1016/j.coastaleng.2007.12.003>, Accessed 2023-05-13. <https://www.sciencedirect.com/science/article/pii/S0378383907001640>.
- Chen, Tianqi, and Carlos Guestrin. 2016. "XGBoost: A Scalable Tree Boosting System." In *Proceedings of the 22nd ACM SIGKDD International Conference on Knowledge Discovery and Data Mining*, KDD '16, New York, NY, USA, August, 785–794. Association for Computing Machinery. Accessed 2023-05-13. <https://dl.acm.org/doi/10.1145/2939672.2939785>.
- Ciavola, Paolo, and Giovanni Coco. 2017. *Coastal Storms: Processes and Impacts*. John Wiley & Sons. Google-Books-ID: ETuKDgAAQBAJ.
- de Andrade, Talia Santos, Paulo Henrique Gomes de Oliveira Sousa, and Eduardo Siegle. 2019. "Vulnerability to beach erosion based on a coastal processes approach." *Applied Geography* 102: 12–19. <https://doi.org/10.1016/j.apgeog.2018.11.003>, Accessed 2023-05-13. <https://www.sciencedirect.com/science/article/pii/S0143622817313127>.
- Dean, R. G., and Cyril J. Galvin Jr. 1976. "Beach erosion: Causes, processes, and remedial measures." *Critical Reviews in Environmental Science and Technology* Publisher: Taylor & Francis Group, <https://doi.org/10.1080/10643387609381643>, Accessed 2023-10-07. <https://www.tandfonline.com/doi/abs/10.1080/10643387609381643>.
- Dean, Robert G. 1991. "Equilibrium Beach Profiles: Characteristics and Applications." *Journal of Coastal Research* 7 (1): 53–84. Publisher: Coastal Education & Research Foundation, Inc., Accessed 2023-06-07. <https://www.jstor.org/stable/4297805>.
- Denner, K., M. R. Phillips, R. E. Jenkins, and T. Thomas. 2015. "A coastal vulnerability and environmental risk assessment of Loughor Estuary, South Wales." *Ocean & Coastal Management* 116: 478–490. <https://doi.org/10.1016/j.ocecoaman.2015.09.002>, Accessed 2023-10-07. <https://www.sciencedirect.com/science/article/pii/S096456911530020X>.
- Dissanayake, Pushpa, Jennifer Brown, and Harshnirie Karunarathna. 2014. "Modelling storm-induced beach/dune evolution: Sefton coast, Liverpool Bay, UK." *Marine Geology* 357: 225–242. <https://doi.org/10.1016/j.margeo.2014.07.013>, Accessed 2023-10-07. <https://www.sciencedirect.com/science/article/pii/S0025322714000801>.

- [sciencedirect.com/science/article/pii/S0025322714002217](https://www.sciencedirect.com/science/article/pii/S0025322714002217).
- Dolan, Robert, and Robert E. Davis. 1994. "Coastal Storm Hazards." *Journal of Coastal Research* 103–114. Publisher: Coastal Education & Research Foundation, Inc., Accessed 2023-10-07. <https://www.jstor.org/stable/25735593>.
- Doukakis, Efstratios. 2005. "Coastal vulnerability and risk parameters." *European Water* 11 (12): 3–7.
- Eichentopf, Sonja, Jos M. Alsina, Marios Christou, Yoshiaki Kuriyama, and Harshnirne Karunaratna. 2020. "Storm sequencing and beach profile variability at Hasaki, Japan." *Marine Geology* 424: 106153. <https://doi.org/10.1016/j.margeo.2020.106153>, Accessed 2023-06-02. <https://www.sciencedirect.com/science/article/pii/S0025322720300414>.
- Elko, Nicole, Tiffany Roberts Briggs, Lindino Benedet, Quin Robertson, Gordon Thomson, Bret M. Webb, and Kimberly Garvey. 2021. "A century of U.S. beach nourishment." *Ocean & Coastal Management* 199: 105406. <https://doi.org/10.1016/j.ocecoaman.2020.105406>, Accessed 2023-10-09. <https://www.sciencedirect.com/science/article/pii/S0964569120303136>.
- Field, C. B., T. F. Stocker, V. R. Barros, D. Qin, K. L. Ebi, and P. M. Midgley. 2011. "IPCC Special Report on Managing the Risks of Extreme Events and Disasters to Advance Climate Change Adaptation." 2011: NH12A–02. Conference Name: AGU Fall Meeting Abstracts ADS Bibcode: 2011AGUFMNH12A..02F, Accessed 2023-05-13. <https://ui.adsabs.harvard.edu/abs/2011AGUFMNH12A..02F>.
- Gallagher, Edith L., Steve Elgar, and R. T. Guza. 1998. "Observations of sand bar evolution on a natural beach." *Journal of Geophysical Research: Oceans* 103 (C2): 3203–3215. <https://doi.org/10.1029/97JC02765>.
- Gornitz, V., T. W. White, and R. M. Cushman. 1991. *Vulnerability of the US to future sea level rise*. Technical Report CONF-910780-1. Oak Ridge National Lab., TN (USA). Accessed 2023-05-13. <https://www.osti.gov/biblio/5875484>.
- Gornitz, Vivien M., Richard C. Daniels, Tammy W. White, and Kevin R. Birdwell. 1994. "The Development of a Coastal Risk Assessment Database: Vulnerability to Sea-Level Rise in the U.S. Southeast." *Journal of Coastal Research* 327–338. Publisher: Coastal Education & Research Foundation, Inc., Accessed 2023-05-13. <https://www.jstor.org/stable/25735608>.
- Greene, Karen. 2002. "Beach nourishment: a review of the biological and physical impacts." Publisher: Atlantic States Marine Fisheries Commission.
- Gunaratna, Thamali, Takayuki Suzuki, and Shinichi Yanagishima. 2019. "Cross-shore grain size and sorting patterns for the bed profile variation at a dissipative beach: Hasaki Coast, Japan." *Marine Geology* 407: 111–120. <https://doi.org/10.1016/j.margeo.2018.10.008>, Accessed 2023-10-08. <https://www.sciencedirect.com/science/article/pii/S002532271730628X>.
- Hallermeier, Robert J. 1980. "A profile zonation for seasonal sand beaches from wave climate." *Coastal Engineering* 4: 253–277. [https://doi.org/10.1016/0378-3839\(80\)90022-8](https://doi.org/10.1016/0378-3839(80)90022-8), Accessed 2023-10-07. <https://www.sciencedirect.com/science/article/pii/0378383980900228>.
- Hanson, H, A Brampton, M Capobianco, H. H Dette, L Hamm, C Lastrup, A Lechuga, and R Spanhoff. 2002. "Beach nourishment projects, practices, and objectivesa European overview." *Coastal Engineering* 47 (2): 81–111. [https://doi.org/10.1016/S0378-3839\(02\)00122-9](https://doi.org/10.1016/S0378-3839(02)00122-9), Accessed 2023-10-09. <https://www.sciencedirect.com/science/article/pii/S0378383902001229>.
- Harley, Mitchell. 2017. "Coastal Storm Definition." In *Coastal Storms*, 1–21. John Wiley & Sons, Ltd. Section: 1 .eprint: <https://onlinelibrary.wiley.com/doi/pdf/10.1002/9781118937099.ch1>, Accessed 2023-05-13. <https://onlinelibrary.wiley.com/doi/abs/10.1002/9781118937099.ch1>.
- Harris, Charles R., K. Jarrod Millman, Stfan J. van der Walt, Ralf Gommers, Pauli Virtanen, David Cournapeau, Eric Wieser, et al. 2020. "Array programming with NumPy." *Nature* 585 (7825): 357–362. Publisher: Springer Science and Business Media LLC, <https://doi.org/10.1038/s41586-020-2649-2>, <https://doi.org/10.1038>/

s41586-020-2649-2.

- Hieu, Phung Dang, Vinh N. Phan, Viet T. Nguyen, Thanh V. Nguyen, and H. Tanaka. 2020. "Numerical study of nearshore hydrodynamics and morphology changes behind offshore breakwaters under actions of waves using a sediment transport model coupled with the SWASH model." *Coastal Engineering Journal* 62 (4): 553–565. Publisher: Taylor & Francis _eprint: <https://doi.org/10.1080/21664250.2020.1828016>, <https://doi.org/10.1080/21664250.2020.1828016>, Accessed 2023-07-06. <https://doi.org/10.1080/21664250.2020.1828016>.
- Hillyer, Theodore M. 1996. *Shoreline Protection and Beach Erosion Control Study: Final Report : an Analysis of the U.S. Army Corps of Engineers Shore Protection Program*. The Institute. Google-Books-ID: LiQYAQAAIAAJ.
- Hoefel, Fernanda, and Steve Elgar. 2003. "Wave-Induced Sediment Transport and Sandbar Migration." *Science* 299 (5614): 1885–1887. Publisher: American Association for the Advancement of Science, <https://doi.org/10.1126/science.1081448>, Accessed 2023-10-08. <https://www.science.org/doi/10.1126/science.1081448>.
- Januait, Rasa, Laurynas Jukna, Darius Jarmalavius, Donatas Pupienis, and Gintautas ilinskas. 2021. "A Novel GIS-Based Approach for Automated Detection of Nearshore Sandbar Morphological Characteristics in Optical Satellite Imagery." *Remote Sensing* 13 (11): 2233. Number: 11 Publisher: Multidisciplinary Digital Publishing Institute, <https://doi.org/10.3390/rs13112233>, Accessed 2023-05-13. <https://www.mdpi.com/2072-4292/13/11/2233>.
- Kantamaneni, Komali, Xiaoping Du, Sainath Aher, and Rao Martand Singh. 2017. "Building Blocks: A Quantitative Approach for Evaluating Coastal Vulnerability." *Water* 9 (12): 905. Number: 12 Publisher: Multidisciplinary Digital Publishing Institute, <https://doi.org/10.3390/w9120905>, Accessed 2023-06-07. <https://www.mdpi.com/2073-4441/9/12/905>.
- Kantamaneni, Komali, Michael Phillips, Tony Thomas, and Rhian Jenkins. 2018. "Assessing coastal vulnerability: Development of a combined physical and economic index." *Ocean & Coastal Management* 158: 164–175. <https://doi.org/10.1016/j.ocemoaman.2018.03.039>, Accessed 2023-06-07. <https://www.sciencedirect.com/science/article/pii/S0964569117304222>.
- Karunarathna, Harshnie, Jose Horrillo-Caraballo, Yoshiaki Kuriyama, Hajime Mase, Roshanka Ranasinghe, and Dominic E. Reeve. 2016. "Linkages between sediment composition, wave climate and beach profile variability at multiple timescales." *Marine Geology* 381: 194–208. <https://doi.org/10.1016/j.margeo.2016.09.012>, Accessed 2023-06-13. <https://www.sciencedirect.com/science/article/pii/S0025322716302146>.
- Katoh, Kazumasa. 1995. "Changes of sand grain distribution in the surf zone." *Proc. Coastal Dynamics '99, Am. Soc. of Eng., New York* 410: 335–364. <https://cir.nii.ac.jp/crid/1571417125673304832>.
- Katoh, Kazumasa. 1997. "Hazaki oceanographical research station (HORS)." *Marine Technology Society. Marine Technology Society Journal* 31 (4): 49. Publisher: Marine Technology Society.
- Kim, Tae-Kon, Changbin Lim, and Jung-Lyul Lee. 2021. "Vulnerability Analysis of Episodic Beach Erosion by Applying Storm Wave Scenarios to a Shoreline Response Model." *Frontiers in Marine Science* 8. Accessed 2023-05-13. <https://www.frontiersin.org/articles/10.3389/fmars.2021.759067>.
- Koroglu, Aysun, Roshanka Ranasinghe, Jos A. Jimnez, and Ali Dastgheib. 2019. "Comparison of Coastal Vulnerability Index applications for Barcelona Province." *Ocean & Coastal Management* 178: 104799. <https://doi.org/10.1016/j.ocemoaman.2019.05.001>, Accessed 2023-05-13. <https://www.sciencedirect.com/science/article/pii/S0964569118308779>.
- Kuriyama, Y. 2002. "Medium-term bar behavior and associated sediment transport at Hasaki, Japan." *Journal of Geophysical Research: Oceans* 107 (C9): 15–15–12. _eprint: <https://onlinelibrary.wiley.com/doi/pdf/10.1029/2001JC000899>, <https://doi.org/10.1029/2001JC000899>, Accessed 2023-10-15. <https://onlinelibrary>.

- wiley.com/doi/abs/10.1029/2001JC000899.
- Lundberg, Scott M, and Su-In Lee. 2017. "A Unified Approach to Interpreting Model Predictions." In *Advances in Neural Information Processing Systems*, edited by I. Guyon, U. Von Luxburg, S. Bengio, H. Wallach, R. Fergus, S. Vishwanathan, and R. Garnett, Vol. 30. Curran Associates, Inc. https://proceedings.neurips.cc/paper_files/paper/2017/file/8a20a8621978632d76c43dfd28b67767-Paper.pdf.
- Mendoza, Ernesto Tonatiuh, Alec Torres-Freyermuth, Elena Ojeda, Gabriela Medelln, Rodolfo Rioja-Nieto, Paulo Salles, and Imen Turki. 2022. "Seasonal changes in beach resilience along an urbanized barrier island." *Frontiers in Marine Science* 9. Accessed 2023-05-23. <https://www.frontiersin.org/articles/10.3389/fmars.2022.889820>.
- Nagai, Toshihiko, and Hideaki Ogawa. 2004. *Annual Report on Nationwide Ocean Wave Information Network for Ports and Harbours (NOWPHAS 2002)*. Technical Report 1069. 3-1-1, Nagase, Yokosuka, 239-0826, Japan. <https://www.pari.go.jp/PDF/3c302621959c63ec768edd5824b631ee9d877e34.pdf>.
- Pape, L., Y. Kuriyama, and B. G. Ruessink. 2010. "Models and scales for cross-shore sandbar migration." *Journal of Geophysical Research: Earth Surface* 115 (F3). <https://doi.org/10.1029/2009JF001644>.
- Pender, Doug, and Harshnirie Karunarathna. 2013. "A statistical-process based approach for modelling beach profile variability." *Coastal Engineering* 81: 19–29. <https://doi.org/10.1016/j.coastaleng.2013.06.006>, Accessed 2023-10-07. <https://www.sciencedirect.com/science/article/pii/S0378383913001142>.
- Perch-Nielsen, Sabine L. 2010. "The vulnerability of beach tourism to climate change index approach." *Climatic Change* 100 (3): 579–606. <https://doi.org/10.1007/s10584-009-9692-1>, Accessed 2023-05-14. <https://doi.org/10.1007/s10584-009-9692-1>.
- Ruessink, B. G., C. Blenkinsopp, J. A. Brinkkemper, B. Castelle, B. Dubarbie, F. Grasso, J. A. Puleo, and T. Lanckriet. 2016. "Sandbar and beach-face evolution on a prototype coarse sandy barrier." *Coastal Engineering* 113: 19–32. <https://doi.org/10.1016/j.coastaleng.2015.11.005>, Accessed 2023-05-13. <https://www.sciencedirect.com/science/article/pii/S0378383915001933>.
- Ruessink, B. G., and Y. Kuriyama. 2008. "Numerical predictability experiments of cross-shore sandbar migration." *Geophysical Research Letters* 35 (1). eprint: <https://onlinelibrary.wiley.com/doi/pdf/10.1029/2007GL032530>, <https://doi.org/10.1029/2007GL032530>, Accessed 2023-10-08. <https://onlinelibrary.wiley.com/doi/abs/10.1029/2007GL032530>.
- SeongYoon, Choi, and E. Yamaji. 2015. "Local-level climate change vulnerability assessment using three indices a case in 4 municipals of Gyeonggi province, Korea." *Journal of Rural Planning* 34 (Special Issue): 261–266. Publisher: Association of Rural Planning, Accessed 2023-06-07. <https://www.cabdirect.org/cabdirect/abstract/20163013841>.
- Suzuki, Takayuki, and Yoshiaki Kuriyama. 2012. "Field Observations of Shoreline Change by Frequency-Banded Wave Energy Flux and Foreshore Shape." *Coastal Engineering Proceedings* (33): 10–10. Number: 33, <https://doi.org/10.9753/icce.v33.posters.10>, Accessed 2023-05-13. <https://icce-ojs-tamu.tdl.org/icce/article/view/6450>.
- Thilakarathne, Salika, Takayuki Suzuki, and Martin Mll. 2023. "Applying Artificial Neural Networks for Predicting Beach Vulnerability to Storm-Induced Erosion." *Journal of JSCE* 11 (2). <https://doi.org/10.2208/journalofjsce.23-18101>.
- Thilakarathne, Salika, Takayuki Suzuki, Martin Mll, Hiroto Higa, and Md Abdul Malek. 2022. "A Simple Approach to Predict the Beach Vulnerability to Storm-induced Erosion in Hasaki Coast, Japan." *Journal of Japan Society of Civil Engineers b2(Coastal Engineering)* 78 (2): 985–990. https://doi.org/10.2208/kaigan.78.2_I_985.
- Turner, Ian L., Mitchell D. Harley, Andrew D. Short, Joshua A. Simmons, Melissa A. Bracs, Matthew S. Phillips, and Kristen D. Splinter. 2016. "A multi-decade dataset of monthly beach profile surveys and inshore wave forcing at Narrabeen, Australia." *Scientific Data* 3 (1): 160024. Number: 1 Publisher: Nature Publishing Group, <https://doi.org/10.1038/sdata.2016.24>, Accessed 2023-05-24. <https://www.nature.com/>

- [articles/sdata201624](#).
- Vidal-Ruiz, Jess Adrin, and Amaia Ruiz de Alegra-Arzaburu. 2019. “Variability of sand-bar morphometrics over three seasonal cycles on a single-barred beach.” *Geomorphology* 333: 61–72. <https://doi.org/10.1016/j.geomorph.2019.02.034>, Accessed 2023-05-13. <https://www.sciencedirect.com/science/article/pii/S0169555X19300765>.
- Virtanen, Pauli, Ralf Gommers, Travis E. Oliphant, Matt Haberland, Tyler Reddy, David Cournapeau, Evgeni Burovski, et al. 2020. “SciPy 1.0: fundamental algorithms for scientific computing in Python.” *Nature Methods* 17 (3): 261–272. Number: 3 Publisher: Nature Publishing Group, <https://doi.org/10.1038/s41592-019-0686-2>, Accessed 2023-05-13. <https://www.nature.com/articles/s41592%E2%80%90019%E2%80%900686%E2%80%902>.
- Zhang, Keqi, Bruce Douglas, and Stephen Leatherman. 2002. “Do Storms Cause Long-Term Beach Erosion along the U.S. East Barrier Coast?” *The Journal of Geology* 110 (4): 493–502. Publisher: The University of Chicago Press, <https://doi.org/10.1086/340633>.
- Zhang, Keqi, Bruce C. Douglas, and Stephen P. Leatherman. 2004. “Global Warming and Coastal Erosion.” *Climatic Change* 64 (1): 41–58. <https://doi.org/10.1023/B:CLIM.0000024690.32682.48>, Accessed 2023-10-08. <https://doi.org/10.1023/B:CLIM.0000024690.32682.48>.